iScience

CellPress
OPEN ACCESS

Article

High contrast ratio optimized total internal reflection prism for compact medium-wave IR target simulation system

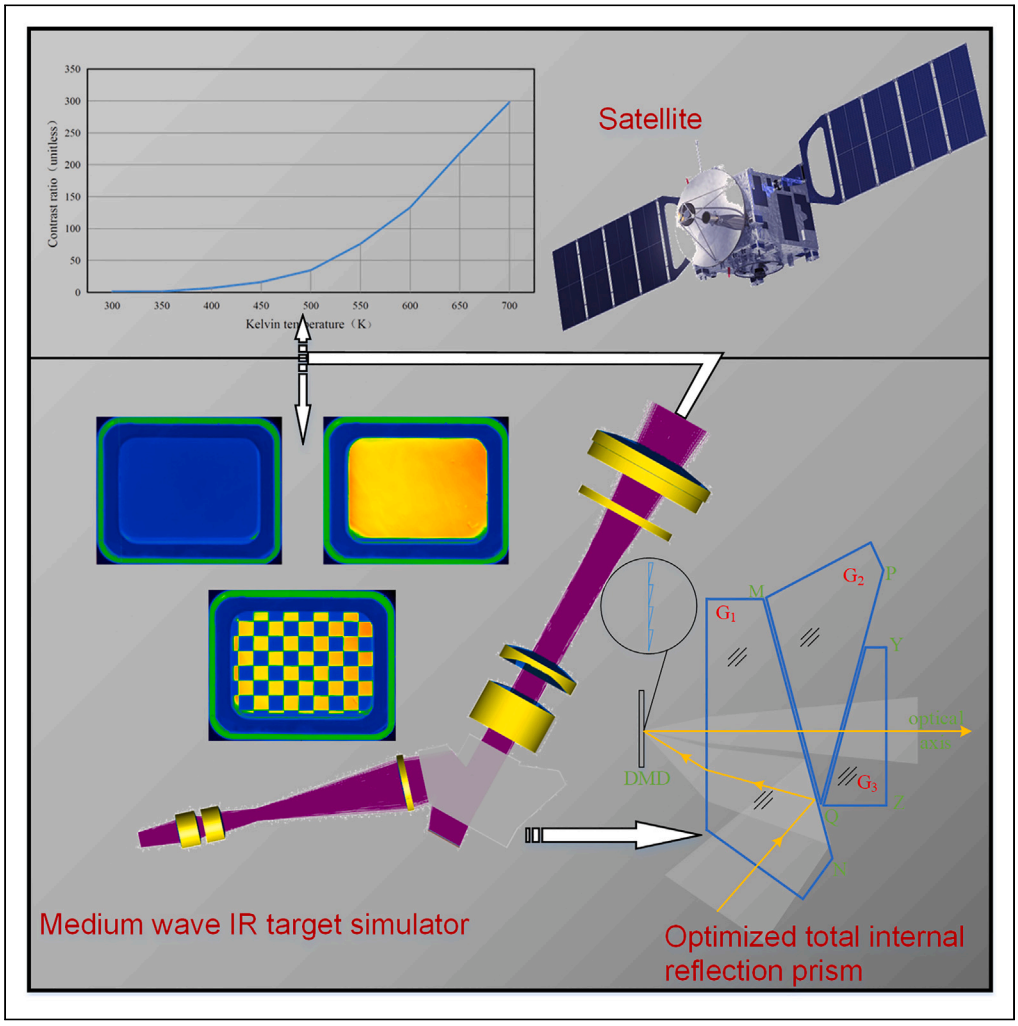

Zongyu Du, Gaofei Sun, Songzhou Yang, Jierui Zhang, Qiang Liu, Yao Meng, Guoyu Zhang

duzongyu2021@163.com

Highlights

Supplement the model between the radiation theory and OTIR prism

The design method of OTIR prism is introduced emphatically

The feasibility of OTIR prism is verified based on Monte Carlo tracing

Du et al., iScience *27*, 108918
February 16, 2024
https://doi.org/10.1016/j.isci.2024.108918

iScience

CellPress
OPEN ACCESS

Article

High contrast ratio optimized total internal reflection prism for compact medium-wave IR target simulation system

Zongyu Du,[1] Gaofei Sun,[1,2,3,4,*] Songzhou Yang,[1,2,3] Jierui Zhang,[1] Qiang Liu,[1] Yao Meng,[1,2,3] and Guoyu Zhang[1,2,3]

SUMMARY

The existing infrared target simulation system with a total internal reflection (TIR) prism has the problem of low imaging contrast ratio, which will seriously affect the quality of the simulated image. This study proposes a design method of optimized TIR prism (OTIR) based on Snell's law in medium-wave infrared (MWIR) to solve the problem. The radiation theory is used to construct the constraint model of the OTIR prism in the MWIR target simulation system. Further, this study investigates the influence of different states of the digital micromirror device on the beam direction and derives the design equation of the OTIR prism composed of three prisms based on Snell's law. Finally, the designed OTIR prism is simulated and experimentally verified. The simulated results show that the OTIR prism of the compact MWIR target simulation system can enhance the contrast ratio. The experimental results show that the output contrast ratio of the simulation system at 700 K is about 298:1. In the specified temperature range, the contrast ratio of the infrared target simulation system increases with the increase of the light source temperature. Thus, the OTIR prism has the function of improving the contrast ratio of MWIR target simulation system.

INTRODUCTION

Infrared target simulation system can simulate the real physical characteristics of targets and is widely used in the ground test of space-borne and missile-borne detection systems.[1–3] As a supplement to visible-light target simulation technology, it can make up for the shortcomings of visible light and laser to a certain extent, meet the requirements of all-weather observation and multi-information collection of the target detection system, and improve the environmental adaptabilities of the target detection system.[4] Imaging contrast ratio is one of the indicators to measure the imaging quality of the rice tissue target simulator, which is related to incident light intensity, display contrast ratio of the digital micromirror device (DMD), optical transfer function of the imaging lens, and so on.[5] DMD-type infrared target simulation system exhibits scattering, reflection, diffraction, and other phenomena, resulting in a significantly reduced contrast ratio of infrared target simulation system, and the imaging performance cannot meet the simulation requirements. With the development of medium-wave infrared (MWIR) detection system,[6–8] how to improve the imaging contrast ratio of MWIR target simulation system has become one of the urgent problems.

In the MWIR target simulation system, the structure of the telecentric optical path has the advantage of high uniformity in the projection image. Moreover, the lower energy utilization can be improved by plating anti-reflection film on the surface of the optical element. Some researchers have studied the contrast ratio of MWIR target simulation system with a telecentric structure. For example, Dupuis et al.[9] developed a DMD infrared scene projector for an infrared tracking system, measured the limiting factors of contrast ratio in the infrared target simulation system, and generated a new concept based on structured illumination of the projector DMD where the structure is dynamically provided by a source-conditioning DMD operating in binary mode. A contrast ratio of 250:1 is reached in the spectral range of 3–5 μm bands and the temperature of 785 K. Beasley et al.[10] gave a detailed overview of the Micromirror Array Projector System (MAPS) of Optical Technology Company of the United States. In the MWIR, a contrast ratio of 90:1 is reached when the DMD is illuminated with a light source temperature of 523 K temperature. Zhang et al.[11] designed a set of infrared dual-band visual simulation optical system based on DMD and realized a dual band and large exit pupil distance of telecentric light path by using direct illumination. When the blackbody temperature is 300° *C*, the minimum and maximum simulated temperatures are 31.6° *C* and 250° *C*, respectively. So the temperature difference is 215.4° *C*, and the normalized contrast ratio of the system reaches 0.98. However, the total internal reflection (TIR) prism structure was not used in the

[1]School of Opto-Electronic Engineering, Changchun University of Science and Technology, Changchun 130022, Jilin, China
[2]Opto-Electronic Measurement and Control Instrumentation, Jilin Province Engineering Research Center, Changchun 130022, Jilin, China
[3]Key Laboratory of Opto-Electronic Measurement and Optical Information Transmission Technology, Ministry of Education, Changchun 130022, Jilin, China
[4]Lead contact
*Correspondence: duzongyu2021@163.com
https://doi.org/10.1016/j.isci.2024.108918

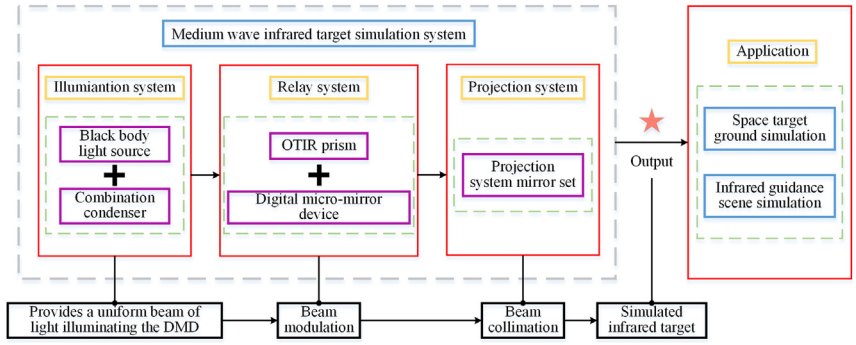

Figure 1. Schematic of the optical system of MWIR target simulation system

aforementioned studies, resulting in the back intercept of the system being too large, which increased the size of the system. Generally, telecentric structures with TIR prisms in infrared target simulation systems are characterized by high homogeneity, facilitate system miniaturization, and allow separate designs of the illumination and projection systems.[12] Some scholars have designed the infrared target simulation system with a telecentric structure of a TIR prism. For example, Pang[13] designed a TIR prism with an imaging contrast ratio of 0.61 normalized to the wavelength band of 3–5 μm and an energy utilization rate of 64.5%. But the corresponding blackbody temperature was not mentioned. The aforementioned research shows that TIR prism can shorten the back intercept and compact the system structure. However, after introducing the TIR prism, the contrast ratio of the system is reduced.

Therefore, this study proposes an OTIR prism for a compact MWIR target simulation system with the background of multi-band target simulators of ultraviolet, visible, MWIR, and long-wave infrared to improve the contrast ratio in the simulation system of the MWIR target and to meet the practical application requirements of the detection system of MWIR target. To improve the contrast ratio of the telecentric structure of TIR prism used in MWIR imaging, the constraint model of the OTIR prism was constructed, the design method of OTIR prism based on Snell's law was proposed, and the OTIR prism of 3–5 μm band was designed. This study reduces the stray light and improves the imaging quality of the MWIR target simulation system. It provides a research idea for improving the contrast ratio of infrared target simulation systems.

RESULTS

Optical system composition of MWIR target simulation

An MWIR target simulation system with a telecentric structure is proposed to improve the contrast ratio of the MWIR target simulation system with TIR prism in the telecentric structure, which mainly consists of a blackbody light source, optical illumination system, relay system (OTIR prism, DMD), and projection system, as shown in Figure 1. The blackbody emits infrared beam. The concentrating prism group is used to converge the beam and shape it. The OTIR prism is used to reduce the system size and derive the DMD off-state beam from the projection system. A DMD is used to simulate the scene target, and the projection system mirror set is used for beam collimation.

The light emitted from the blackbody is concentrated by the optical illumination system and then directed into the OTIR prism and uniformly illuminates the DMD. The DMD simulates the MWIR target, and the projection system collimates the simulated target to form parallel light, which is provided to the MWIR target detection system for functional detection.

Principle of TIR prism and design idea of OTIR prism

The angle between the illumination and projection beam is limited by the deflection angle of DMD. It is easy to cause some edge rays of the two beams to overlap and interfere with each other, and also easy to cause mutual blocking. To avoid the aforementioned situation, the optical splitting system must be added to ensure the compact structure and the rationality of the system's optical path. The splitting of TIR prism generally uses two prism structures, as shown in Figure 2. From the deflection characteristics of the DMD,[14] the angle between the incident and reflected rays is 24° after the light is modulated by the DMD. i_c is the critical angle of total reflection of the prism material. The light will be fully reflected to the DMD when the angle of incidence at the prism slope is greater than i_c. At the same time, it is also necessary to ensure that the projection beam modulated by the DMD is transmitted through the prism, and the angle of incidence of any light in the projection beam when it passes through the prism again is less than the critical angle; i.e., when $i_1 < i_2 < i_c$ is satisfied, the light can be transmitted through.

It is well known that the micromirror on the DMD has three working states, i.e., on-state, flat-state, and off-state.[15] Although the flat-state is inactive, there is still a short time zero position when the micromirror changes from the on-state to the off-state. During DMD operation, the surrounding non-working area of DMD can also be considered a flat-state. The protective glass of DMD reflects the light beam and can also be regarded as flat-state. In addition, the hinges below the DMD can create scattered light in the projection system. These factors introduce stray light into the optical system and reduce the contrast ratio. The F-number of the infrared target simulator projection system is usually between 2.4 and 3, and corresponding beam aperture angle is 9.4°–11.7°. The TIR prism will cause the flat and scattered beams, etc., to enter the projection system. Therefore, the OTIR prism should be improved based on TIR prism function to realize that the beam in flat-state and off-state is far away from the projection system and enhance the contrast ratio of the infrared target simulator.

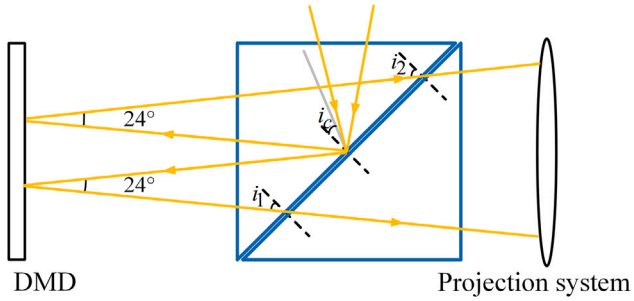

Figure 2. Schematic diagram of TIR prism

Constraint model construction of OTIR prism

To improve the contrast ratio of the MWIR target simulation system, the relationship between the contrast ratio and the constraint model of the OTIR prism needs to be clarified. Contrast ratio is usually calculated in two ways: the OFF/ON (FO) contrast ratio and the American National Standards Institute (ANSI) contrast ratio. The FO contrast ratio is more suitable for a dynamic projection system, where the contrast ratio C is Equation 1, defined as the ratio of the luminosity or luminous flux of a display that is all white to all black.

$$C = \frac{L_{on}}{L_{off}} \quad \text{(Equation 1)}$$

where C is the contrast ratio, L_{on} is the output brightness of the all-white screen, and L_{off} is the output brightness of the all-black screen.

It can be seen that when L_{on} alone increases, L_{off} alone decreases, or both occur at the same time, the higher the contrast C, the greater the difference between light and dark in the simulated image. To improve the contrast ratio of the system, the radiation brightness of the background light should be reduced when the target brightness is constant. Since the background light intensity usually reaches the system image plane by scattering and reflection, its energy transmission process is consistent with the basic radiation transmission theory. The fundamental radiation transmission of the background light energy is shown in Figure 3.

The meta-illuminated area $d\Phi_2$ received by the illuminated surface dA_1 emitted by the radiation flux dA_2 is given by Equation 2.

$$d\Phi_2 = \left(\cos\varphi_1 \frac{dA_2 \cos\varphi_2}{r^2}\right) \frac{L_1}{E_1} E_1 dA_1 = GCF \cdot BSDF \cdot d\Phi_1 \quad \text{(Equation 2)}$$

where L_1 is the radiation luminance of the meta-illuminated area, φ_1 is the angle between the normal line of the microfacet and the center line, φ_2 is the angle between the normal line of the receiving microfacet and the central line, r is the length of the connection between the center of two microfacets, GCF is the solid angle of the light source microfacet to the receiving microfacet, BSDF is the surface bidirectional scattering distribution function, $d\Phi_1$ is the radiation flux of the light source surface, and E_1 is the irradiance of the source microfacet.

To suppress the background brightness and improve the contrast ratio, it is necessary to reduce the receiving radiation flux $d\Phi_2$ of microfacet. This can be achieved by lowering GCF. The GCF value of stray light transmission at each stage is reduced by setting stray light suppression structures such as shading, blocking rings, and eliminating stray light diaphragm.[16] In this study, we design an OTIR prism based on the Snell principle to achieve the modulation of the DMD off-state and flat-state beam to reduce the GCF, reduce the brightness of background radiation L_{off}, and improve the contrast ratio C of the system. The comparison between the TIR prism and the OTIR prism principle that enhances the contrast ratio is shown in Figure 4.

According to the modulation principle of the DMD,[17,18] combined with the requirements of the illumination system and projection system in the design of TIR prism,[19,20] the contrast ratio enhancing OTIR prism should meet the following three conditions.

(1) The light beam of the illumination system can be fully reflected in the OTIR prism and uniformly illuminate the DMD, which can pass through the OTIR prism into the projection system after being reflected by the DMD.
(2) The off-state and flat-state beam, which meet total reflection on the OTIR prism, are far away from the projection system, and the on-state beam refracts enter the projection system when the DMD-reflected beam passes through the OTIR prism.
(3)The light beam entering the projection system should be parallel to the DMD optical axis.

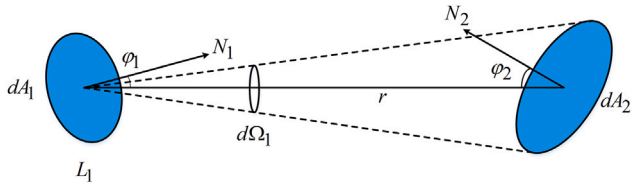

Figure 3. Schematic diagram of basic radiation transmission

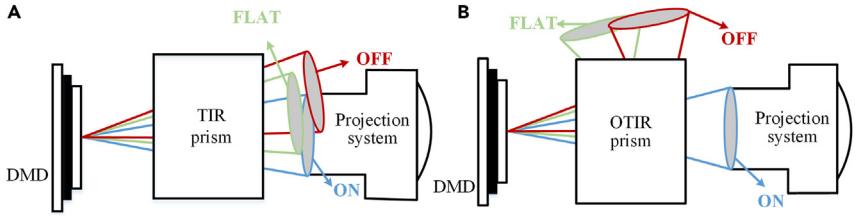

Figure 4. Principle comparison between TIR prism and OTIR prism

(A) TIR prism.

(B) OTIR prism.

The beveled edge angle of OTIR prisms generally refers to the second surface of the DMD-reflected beam passing through the prism and the direction of the perpendicular DMD optical axis, which mainly relies on this beveled edge angle to achieve the function. Owing to the fact that hypotenuse angle of the OTIR prism cannot simultaneously meet the aforementioned conditions, according to the analysis, the design of at least three prisms is needed to improve the contrast ratio of the OTIR prism.

OTIR prism angle design theory

The prism angle of the beveled edge determines the direction of the beam modulation. The first OTIR prism is used to turn the beam irradiated by the illumination system and uniformly illuminate the DMD. The second prism is used to modulate the beam direction of DMD in the off-state, flat-state, or on-state. The third prism is used to orient the beam from the OTIR prism parallel to the DMD optical axis to ensure it enters the projection system.

The primary purpose of the first prism G_1 is to uniformly illuminate the DMD with the incident light from the illumination system, as shown in Figure 5A. The angle θ_1 of the beveled edge of the prism has to satisfy two conditions, i.e., the upper edge light ray AB incident to the beam on the beveled edge of the MN should have an angle of incidence η_1 greater than the critical angle and the lower edge light ray CD, which is reflected from the beam via the DMD, has an angle of incidence η_2 to the bevel MN that is less than the critical angle.

The light cone angle of the illumination beam incident on the DMD is $\arctan\left(\frac{1}{2F}\right)$, and the angle between the illumination beam's upper edge and the projection system's optical axis is $2\theta_{DMD} - \arctan\left(\frac{1}{2F}\right)$. The angle becomes $\arctan\left(\frac{1}{2F}\right)$ after the reflection in the on-state of the DMD. When the beam is first incident on the beveled MN, Snell's law and total reflection condition can be used to calculate that Equation 3 should be satisfied. Similarly, by calculating the conditions that should be satisfied by the beam reflected from the DMD into the beveled MN, it can be concluded that the beveled edge angle θ_1 of the first prism should satisfy Equation 4, as follows:

$$\theta_1 = \arcsin\frac{n_a}{n_{g\,\min}} - \arcsin\frac{2\theta_{DMD} - \arctan\left(\frac{1}{2F}\right)}{n_{g\,\min}} \quad \text{(Equation 3)}$$

$$\arcsin\frac{n_a}{n_{g\,\min}} - \arcsin\frac{2\theta_{DMD} - \arctan\left(\frac{1}{2F}\right)}{n_{g\,\min}} \le \theta_1 \le \arcsin\frac{n_a}{n_{g\,\max}} - \arcsin\frac{\arctan\left(\frac{1}{2F}\right)}{n_{g\,\max}} \quad \text{(Equation 4)}$$

where θ_1 is the beveled edge angle of the first prism; n_a is the refractive index of air, $n_{g\,\min}$ and $n_{g\,\max}$ are the minimum and maximum refractive indices of the prism material at 3–5 μm, respectively; θ_{DMD} is the deflection angle of DMD; and F is the F-number of the system.

The second prism G_2 is the essence of the OTIR prism that distinguishes it from the TIR prism and is designed to realize the beam modulation of DMD on-state and off-state. Figures 5B and 5C show the beam direction of the DMD in the on-state and off-state, respectively. There are two incident bevels for the light, one of which is parallel to the bevel MN of G_1, with a certain air interval in the middle, so all the DMD-modulated light can pass through this bevels. The second bevel PQ plays the role of modulating the beam. The design of the bevel angle of G_2 is similar to the principle of the first prism G_1. The angle I between the lower edge of the light reflected by the DMD and the optical axis is given by Equation 5. According to Snell's law, the angle θ_2 of the beveled of the second prism can be derived as Equation 6, as follows:

$$I = 2\theta_{DMD} + \left(2\theta_{DMD} - \arctan\left(\frac{1}{2F}\right)\right) \quad \text{(Equation 5)}$$

$$\theta_2 = \arcsin\frac{1}{n_{\max}} - \arcsin\frac{4\theta_{DMD} - \arctan\left(\frac{1}{2F}\right)}{n_{\max}} \quad \text{(Equation 6)}$$

where θ_2 is the second prism beveled edge PQ angle.

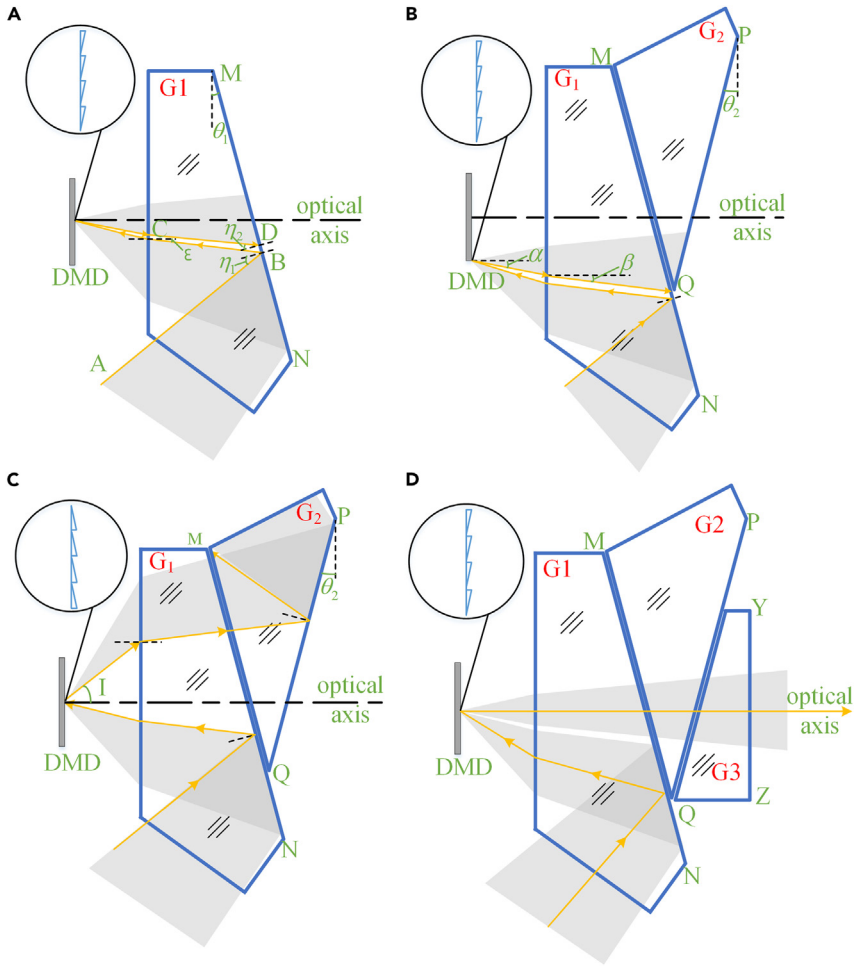

Figure 5. Schematic design of prism angle

(A) First prism.

(B) The second prism of the DMD on-state.

(C) The second prism of the DMD off-state.

(D) Third prism.

The third prism G_3 ensures that the main light is parallel to the DMD optical axis. The side of the prism near the beveled edge of the second prism is inclined, parallel to the inclined plane PQ of the second prism, with a certain air interval in the middle, and the other side should be perpendicular to the optical axis. The beam direction in the on-state of the DMD is shown in Figure 5D.

The OTIR prism angle's design can determine the beam's optical path direction. In the MWIR target simulation system based on Snell's law, the angle between the upper edge of the illumination beam and the optical axis of the projection system is related to the F-number of the system. The aforementioned equations are applied to infrared target simulation systems with different prism materials and F-numbers.

OTIR prism thickness design theory

During the design process of the OTIR prism, thickness is also an important parameter. A too thick prism will not only cause the loss of light energy but also increase the working distance of the projection system. A prism that is too thin illumination cannot fully illuminate the DMD, which is equivalent to reducing the size of the DMD and will change the resolution of the target simulation system, which is not allowed.

The central wavelength is used to design the thickness of prism G_1. The angle of the lower edge ray with the central wavelength is analyzed as $2\theta_{DMD} - \arctan\left(\frac{1}{2F}\right)$. As shown in Figure 6A, when the ray EF is incident along the lower edge of DMD, the fully reflected light is reflected exactly to the upper edge G of the DMD. It is considered that this is the minimum thickness of the OTIR prism, and the thickness L_1 of the first prism can be calculated as Equations 7 and 8, as follows:

$$L_1 = KH = KJ + HJ = GX + HJ \quad \text{(Equation 7)}$$

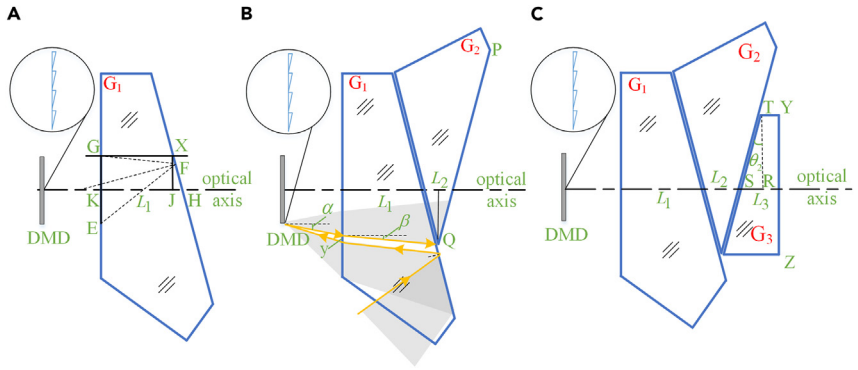

Figure 6. Schematic design of prism thickness

(A) First prism.

(B) Second prism.

(C) Third prism.

$$L_1 = \frac{D}{\tan(2\theta_1+\varepsilon)+\tan\varepsilon} + \frac{D}{2}\cdot\tan\theta_1 \quad \text{(Equation 8)}$$

where D is the diagonal line length of DMD and ε is the refraction angle corresponding to the central wavelength.

For the thickness G_2, to avoid the actual machining and adjustment, the edge of the Q point perpendicular to the plane is involved in imaging on the image plane, affecting the imaging contrast ratio. Therefore, this study uses the DMD on-state of the upper edge light. To determine the thickness of the second prism, the position y needs to be determined, as shown in Figure 6B. According to the geometric relation, y and the thickness of the second prism L_2 can be derived as Equations 9 and 10, respectively.

$$y = \frac{\frac{y}{\tan(\beta)} - L_1}{\tan\theta_0} - \frac{D}{2} - l\tan\alpha \quad \text{(Equation 9)}$$

$$L_2 = \frac{2y}{\tan(\beta)} - 2L_1 \quad \text{(Equation 10)}$$

where l is the distance between DMD and prism, β is the included angle between the light reflected to the lower edge of the second prism and the optical axis of DMD, $\beta = \arcsin\frac{\arctan\left(\frac{1}{2F}\right)}{2.2}$, and α is the angle between the reflected light and the optical axis at the lower edge of DMD.

According to the geometric relation, as shown in Figure 6C, the thickness L_3 of G_3 is given by Equation 11.

$$L_3 = d_0\tan\theta_2 + l_0 \quad \text{(Equation 11)}$$

where d_0 is the distance of TR and l_0 is the distance of TY in Figure 6C.

Using Equations 3, 4, 5, 6, 7, 8, 9, 10, and 11, the model of OTIR prism with improved contrast ratio can be calculated by substituting the corresponding data. In this way, all the on-state beams reflected by DMD enter the projection system. However, the flat-state and off-state beams reflected by DMD are all reflected on the second surface of the prism G_2 and move away from the projection system.

DISCUSSION

Contrast ratio simulation analysis of OTIR prism

ZnS is chosen as the material for the design of the OTIR prism with a compact refractive index in the band of 3–5 μm. Combined with the design index of the MWIR target simulator, the F-number of the system is 2.633, the diagonal length of DMD is 17.78 mm, and the deflection angle is $\pm 12°$. Since the DMD is composed of millions of image elements, to fit the reality in the simulation, the surface microstructure of the DMD is deflected by $\pm 12°$ using a scale structure in the simulation software. As shown in Figure 7, the designed infrared target simulation system was constructed by TracePro software when θ_2 is in a certain angle and the DMD is in the on-state.

Energy utilization is another factor to measure the OTIR prism in addition to contrast ratio, which should be considered in the study. The energy utilization rate of the OTIR prism is closely related to the optical efficiency of the whole system and is mainly affected by the energy utilization rate of the internal and external surfaces of the prism and the thickness of the prism on the light energy absorption. The energy utilization rate τ of the OTIR prism is shown in Equation 12.

$$\tau = \tau_1^4 \times \tau_2^4 \times (1 - \tau_3) \quad \text{(Equation 12)}$$

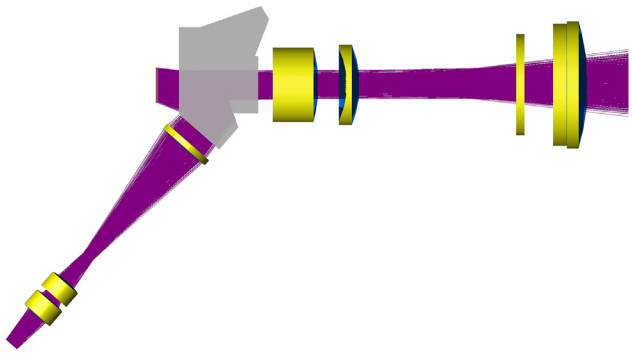

Figure 7. TracePro simulation diagram of MWIR target simulation system

where τ_1 is the transmittance of the outer surface of the OTIR prism, τ_2 is the transmittance of the inner surface of the OTIR prism, and τ_3 is the light energy loss of the thickness of the OTIR prism.

The energy utilization rate of the outer surface of the OTIR prism is mainly affected by the anti-reflection film, which is taken to have a transmission rate of 98%. The loss of the beam passing through the inner surface of the OTIR prism through the air layer is relatively high, with a transmission rate of about 97% on each side.[21] The thickness of the OTIR prism will also affect its energy absorption, with a decrease in energy utilization rate as the prism thickness increases.

As θ_2 increases, more light from flat-state is reflected by the second surface of the second OTIR prism, with the higher contrast ratio. However, the L_2 also increases, and the energy utilization decreases. In infrared systems, the FO contrast ratio is also calculated by the ratio of luminous flux. Combining the contrast ratio equation and tracing 100,000 rays in the simulation software, the relationship between the contrast ratio and energy utilization ratio of the infrared target simulation system with θ_2 was obtained, as shown in Figure 8.

It can be seen from the figure that the second prism does not exist when $\theta_2 = 0^\circ$. The corresponding structure is the two-block TIR prism. The contrast ratio of the system is lower at this point, but the energy utilization is higher. With the increase of the angle of the second OTIR prism, the contrast ratio of the infrared target simulation system also increases. And when it increases to a certain value, the contrast ratio reaches a maximum value and remains constant. On the contrary, the energy utilization of the target simulation system decreases with the increase of the angle of the second OTIR prism, but the range of change is compact.

It shows that the OTIR prism can enhance the contrast ratio of the system. The designed parameters are substituted into the equations in section 3, while a certain air spacing, typically less than 10 μm, is left between each prism to prevent scattering.[22] Owing to the limitation of the manufacturing process, the air interval $\Delta = 0.001mm$ is designed in this study. Considering the processing difficulty of the OTIR prism and the design requirements of the MWIR target simulation system, the design results of the OTIR prism are shown in Table 1. Figure 9 shows the simulated beam directions for different states of the DMD in the IR target simulator according to the design results in Table 1. Figures 9A–9C correspond to the simulation results when the surface micromirror of the DMD is +12°, 0°, and −12°, respectively.

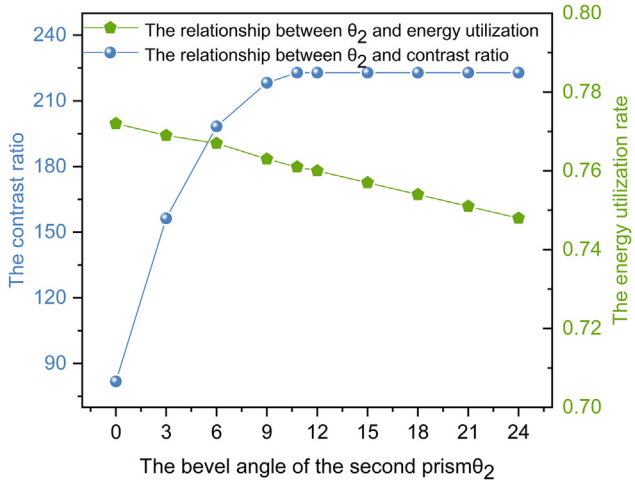

Figure 8. Relation curves of contrast ratio, energy utilization ratio and θ_2

Table 1. Design parameters of OTIR prism

Prism serial number	θ_i	L_i
1	21°	22 mm
2	21°	13.430 mm
3	0°	6.720 mm

In the simulation software, the DMD is used as the image plane in the illumination optical system, and the uniformity of the image plane should be ensured, so the simulated image plane is larger than the actual image plane. The light threshold is set to 0.1, showing the high-energy light's path. It can be seen from the figure that the on-state beam enters the projection system, while the flat-state and off-state beams are far away from the projection system.

Experimental verification

The system is experimentally verified to verify the imaging contrast ratio of the MWIR target simulation system. Figure 10A shows the physical diagram of the OTIR prism with improved contrast ratio, and the physical diagram of the MWIR target simulation system is shown in Figure 10B after the system is installed.

An MWIR thermal imager was used to test the infrared target simulation system for the experiment. The temperature of the thermal imager ranges from −10°C to +1,200°C. The temperature of the light source ranges (room temperature) from +20°C to +700°C. To avoid deviations caused by external environmental factors, each time the temperature of the light source is changed, the measurement is carried out after the temperature of the light source is stabilized (during the experiment, the measurement is carried out at an interval of 5 min after the light source is raised to the specified temperature). At the same time, to avoid measurement errors, the contrast ratio on different temperature values is measured repeatedly. The experimental measurement data are substituted into Equation 1, and the relationship between the imaging contrast ratio of the system and the variation of the blackbody temperature at different temperature values is obtained by combining Planck's formula, as shown in Figure 11.

When the blackbody is set to 300 K, the high temperature and low temperature of the output image of the MWIR target simulation system are 294.63 K and 292.07 K, respectively. The contrast ratio is 1.113:1. When the blackbody is set to 700 K, the high temperature and low temperature of the output image of the MWIR target simulation system are 576.82 K and 301.5 K, respectively, and the contrast ratio is 298.025:1. The background temperature drifted by 9.43 K during this process, indicating that the influence of stray light was compact. It can be seen from the experimental results that the contrast ratio of the telecentric structure with the OTIR prism is improved compared with other structures of the MWIR target simulation system.[9,10] Figure 12 shows the simulated images of DMD in full-on and full-off state at 700 K and the output images of the simulated system with black and white grid input. The test results show that the optical system designed in this study can fully meet the requirements of MWIR target detection systems.

Conclusion

This study proposed a design method for OTIR prism to improve the contrast ratio of MWIR target simulation system with the TIR prism telocentric structure based on Snell's law. The design model of OTIR prism for improving contrast ratio is constructed from the perspective of the radiation principle. A three-block OTIR prism with an energy utilization rate of 75.1% is designed to achieve that the DMD off-state and flat-state beams are totally reflected and away from the projection system while the on-state beams are refracted and enter the projection system. It solves the problem of partial stray light entering the projection system, thus improving the contrast ratio of the MWIR target simulation system with the telocentric structure of the TIR prism. The simulation results showed that, as the angle of the second

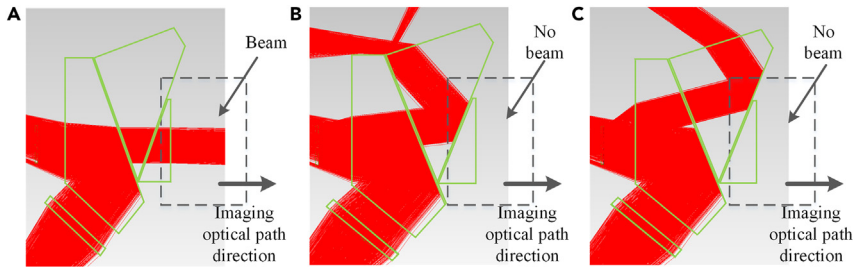

Figure 9. Beam tracing results on different DMD states

(A) on-state.

(B) flat-state.

(C) off-state.

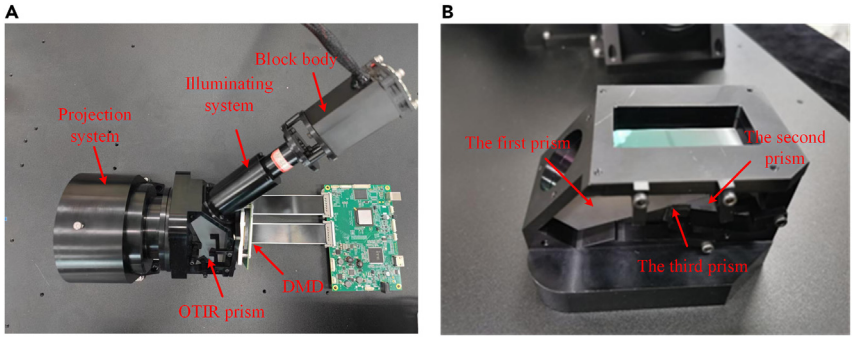

Figure 10. Physical picture
(A) OTIR prism.
(B) MWIR target simulation system.

prism increases, the contrast ratio of the MWIR target simulation system also gradually increases to a certain value, which has the effect of enhancing the contrast ratio. The experimental analysis showed that the contrast ratio of the MWIR target simulation system increases with the increase of the temperature of the light source at 300–800 K. When the temperature is 700 K, the contrast ratio of the system is about 298:1. The imaging effect of the MWIR target simulation system has been improved, and it has the characteristics of high contrast ratio. This design provides a theoretical basis for the design of an infrared target simulation system. The infrared target simulation system based on OTIR can be widely used in the ground detection of infrared target detection systems, multi-spectral detection systems, and other infrared detection systems.

Limitations of study

The diffraction phenomenon of DMD reflects different levels of light, which reduces the contrast. The wavelength of the present design in this study is 3–5 μm, which is about 5 times different from the single-pixel image element of the DMD, but it will still be slightly affected. With the gradual miniaturization of single-pixel image elements of spatial light modulation devices, the diffraction phenomenon will become more and more obvious. In order to better improve the contrast of the target simulation system, the diffraction phenomenon needs to be quantitatively analyzed and studied in the future.

STAR★METHODS

Detailed methods are provided in the online version of this paper and include the following:

- KEY RESOURCES TABLE
- RESOURCE AVAILABILITY
  - Lead contact

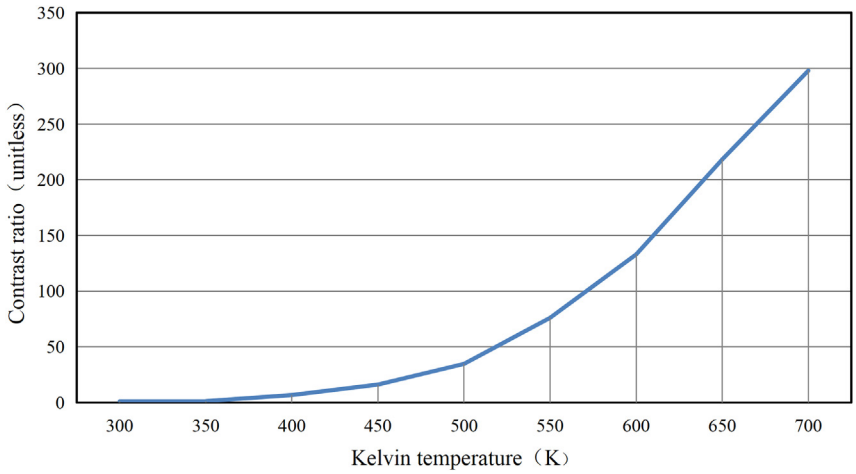

Figure 11. Contrast ratio curve with blackbody temperature

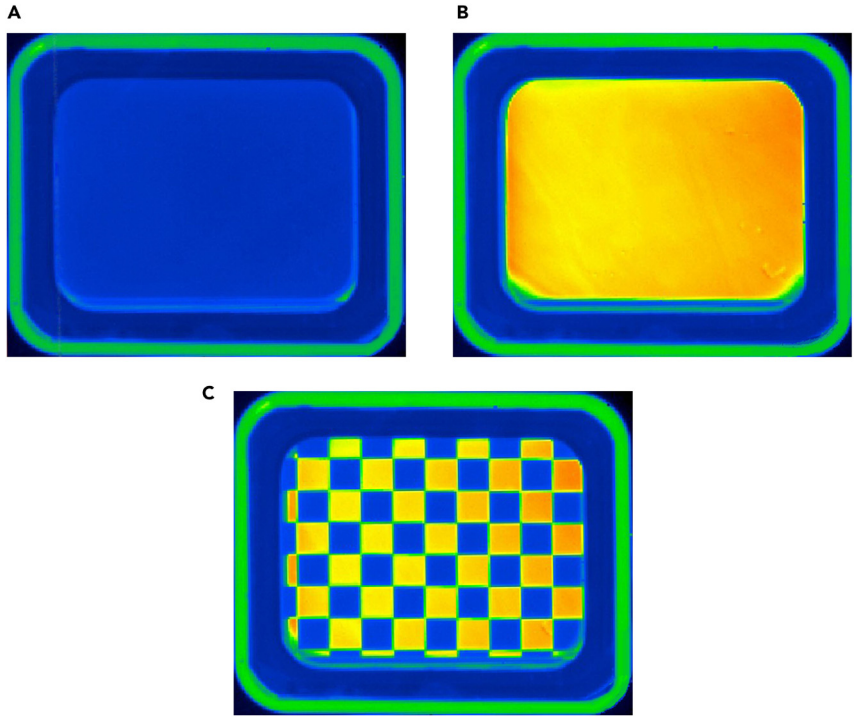

Figure 12. Output image of simulation system at 700 K

(A) DMD is full-off state.

(B) DMD is full-on state.

(C) Input is black and white grid image.

ACKNOWLEDGMENTS

This work was supported by the 111 Project of China (D21009), National Natural Science Foundation of China (61703057), Science and Technology Development Program of Jilin Province (20210201034GX), and Jilin Province Innovation and Entrepreneurship Talent Funding Project (2023QN13).

AUTHOR CONTRIBUTIONS

Conceptualization, methodology, formal analysis, writing – original draft, visualization, Z.D., G.S., and S.Y.; writing – review & editing, Z.D. and S.Y.; investigation, J.Z., Y.M., and Q.L.; project administration, funding acquisition, G.S., G.Z., and S.Y.

DECLARATION OF INTERESTS

The authors declare no competing interests.

Received: August 18, 2023
Revised: November 14, 2023
Accepted: January 11, 2024
Published: January 15, 2024

REFERENCES

1. López-Alonso, J.M., José, M.L., Brian, M., Arthur, R.W., Guy, Z., Daniel, M., and Glenn, D.B. (2005). Characterization of digital-micromirror device-based infrared scene projector. Opt. Eng. *44*, 086402.
2. Du, Z., Sun, G., Yang, S., Zhang, J., Meng, Y., and Liu, Q. (2023). Design of an optical illumination system for a long wave infrared scene projector based on diffraction characteristics. Opt Express *31*, 30267–30284.
3. Pan, Y., Hu, M., Xu, X., and Qiao, Y. (2020). Opto-mechanical temperature adaptability analysis of a dual-band IRSP for HWIL simulation. Infrared Phys. Technol. *105*, 103164.
4. Zheng, R., Li, C., Gao, Y., Li, G., Liu, B., and Sun, K. (2022). Design of optical system of infrared star simulator uniform radiation under specific irradiance. Acta Photonica Sin. *51*, 24–32.
5. Chen, X., and Jiang, A. (2019). Source simulation experimental system based on digital micromirror device. Acta Opt. Sin. *39*, 178–185.
6. Wu, Z., and Wang, X. (2020). Stray light correction for medium wave infrared focal plane array-based compressive imaging. Opt Express *28*, 19097–19112.
7. Rogalski, A. (2011). Recent progress in infrared detector technologies. Infrared Phys. Technol. *54*, 136–154.
8. Cao, J., Chang, J., Huang, Y., Wu, Y., Ji, Z., Lai, X., Wang, J., Li, Y., Zhu, W., and Li, X. (2023). Optical design and fabrication of a common-aperature multispectral imaging system for integrated deep space navigation and detection. Opt Laser. Eng. *167*, 107619.
9. Dupuis, J.R., Mansur, D.J., Grant, S., and Newbry, S.P. (2012). Contrast ratio analysis for DMD-based IR scene projector. Proc. SPIE *8356*, 19–29.
10. Beasley, D.B., Bender, M., Crosby, J., McCall, S., Messer, T., and Saylor, D.A. (2005). Advancements in the micromirror array projector technology II. Proc. SPIE *5785*, 68–79.
11. Zhang, J.Z., Guo, B.H., Tan, X.Q., and Sun, Q. (2013). Design and testing of high contrast ratio MW/LW infrared dual-bands scene simulation system. Infrared Laser Eng. *42*, 2894–2900.
12. Song, Y.S., Yang, J.F., Zhao, Y.Y., Yan, X.T., and Ma, X.L. (2015). Optical System Design for Infrared Target Simulator. Acta Opt. Sin. *35*, 338–345.
13. Pang, G.N. (2018). Key Technology on DMD Based Infrared Scene Simulation (Changchun University of Science and Technology).
14. Li, Q.K., Xiao, Y., Liu, H., Zhang, H.L., Xu, J., and Li, J.H. (2019). Analysis and correction of the distortion error in a DMD based scanning lithography system. Opt Commun. *434*, 1–6.
15. Meuret, Y., and Visschere, P.D. (2003). Contrast ratio-improving methods for Digital Micromirror Device projectors. Opt. Eng. *42*, 840–845.
16. Wang, H., Chen, Q.F., Ma, Z.P., Yan, H.Y., Lin, S.M., and Xue, Y.K. (2022). Development and Prospect of Stray Light Suppression and Evaluation Technology. Acta Photonica Sin. *51*, 125–180.
17. Fu, S., Xing, F., and You, Z. (2021). DMD-based image-free system for real-time detection and positioning of point targets. Opt Express *29*, 41268–41281.
18. Lee, B. (2018). Introduction to ±12 Degree Orthogonal Digital Micromirror Devices (DMDs) (Texas Instrument Incorporated), pp. 1–4.
19. Bai, X., Jing, X., and Liao, N. (2021). Design method for the high optical efficiency and uniformity illumination system of the projector. Opt Express *29*, 12502–12515.
20. Huang, Y.C., and Pan, J.W. (2014). High contrast ratio and compact sized prism for DLP projection system. Opt Express *22*, 17016–17029.
21. Qiao, Y., Xu, X., Pan, Y., and Li, Y. (2014). Research on DMD infrared scene projector with a high contrast ratio infrared prism design. Optik *125* (22), 6854–6859.
22. Single-Panel DLP TM Projection System Optics (2005). Application report Texas Instrument. www.ti.com.

STAR★METHODS

KEY RESOURCES TABLE

REAGENT or RESOURCE	SOURCE	IDENTIFIER
Software and algorithms		
OpticStudio	Zemax	Zemax
Tracepro	Lambda Research	Tracepro

RESOURCE AVAILABILITY

Lead contact

Further information and requests for resources, measurement procedures and data can be directed to the lead contact, Gaofei Sun (duzongyu2021@163.com).

Materials availability

This study did not generate new unique reagents.

Data and code availability

- All data reported in this paper will be shared by the lead contact upon request.
- The codes are available on reasonable request from the lead contact.
- Any additional information required to reanalyze the data reported in this paper is available from the lead contact upon request.

METHOD DETAILS

Nomenclature and units	
C	contrast ratio [/]
L_{on}	output brightness of the all-white screen [cd/m^2]
L_{off}	output brightness of the all-black screen [cd/m^2]
dA_1	meta-illuminated area [m^2]
dA_2	illuminated surface [m^2]
$d\Phi_2$	radiation flux [lm]
L_1	radiation luminance of the meta-illuminated area [cd/m^2]
φ_1	angle between the normal line of the microfacet and the center line [°]
φ_2	angle between the normal line of the receiving microfacet and the central line [°]
R	length of the connection between the center of two microfacets [m]
GCF	solid angle of the light source microfacet to the receiving microfacet [°]
BSDF	surface bidirectional scattering distribution function [/]
$d\Phi_1$	radiation flux of the light source surface [lm]
E_1	irradiance of the source microfacet [W/m^2]

(*Continued on next page*)

Continued

Nomenclature and units	
G_1	First prism [/]
G_2	Second prism [/]
G_3	Third prism [/]
θ_1	beveled edge angle of the first prism [°]
n_a	refractive index of air [/]
$n_{g\ min}$	minimum refractive index of the prism material at 3-5μm [/]
$n_{g\ max}$	maximum refractive index of the prism material at 3-5μm [/]
θ_{DMD}	deflection angle of DMD [°]
F	F-number of the system [/]
θ_2	second prism beveled edge angle [°]
MN	Beveled edge of first prism [/]
PQ	Beveled edge of second prism [/]
YZ	Beveled edge of third prism [/]
D	diagonal line length of DMD [mm]
ε	refraction angle corresponding to the central wavelength [°]
l	distance between DMD and prism [mm]
β	ncluded angle between the light reflected to the lower edge of the second prism and the optical axis of DMD [°]
α	angle between the reflected light and the optical axis at the lower edge of DMD [°]
τ	energy utilization rate of the OTIR prism [%]
τ_1	transmittance of the outer surface of the OTIR prism [%]
τ_2	transmittance of the inner surface of the OTIR prism [%]
τ_3	light energy loss of the thickness of the OTIR prism [%]

Modeling

The modeling experiments were conducted mainly on the TracePro optical software developed by Lambda Research, Inc. in the United States. The lenses of the illumination optical system and projection optical system designed using Zemax software were imported into Tracepro.

Firstly, we study the radiation theory and construct the constraint model of OTIR prism in the MWIR target simulation system; we analyze the influence of different states of DMD on the beam direction, derive the design equation of OTIR prism composed of three prisms based on Sneer's law, and design the main parameter and profile of OTIR prism. (Figures 5A–5D and 6).

Second, the designed OTIR prism was simulated in Tracepro. Both the illumination optics and projection optics designed in Zeamx were imported into Tracepro and jointly simulated with the OTIR. Through the simulation, the overall shape of the OTIR prism is determined first to avoid the effect on the beam due to the aperture of the OTIR prism. It should be noted that the surface and material properties of the lens will be lost during the import process, and the material of the prism needs to be set to match the refractive index and Abbe number in Zemax. Also set the surface transmittance of the lens and prism. And the scale structure (i.e., surface micro-reflector) is set for the DMD to simulate the real deflection of the DMD by setting the scale structure. Next, the simulation of the second prism of the OTIR prism at different angles obtained different contrast results (Figure 8), to determine that the simulation is consistent with the actual calculation results, so as to determine the model of the OTIR prism.

After determining the model

Monte Carlo ray tracing method is used. Monte Carlo ray tracing is a probability-based statistical algorithm that simulates the propagation of light rays through a scene by randomly sampling the rays to achieve realistic scene rendering. The number of rays is chosen to take into account both "the more rays the more realistic" and "the number of rays does not significantly improve the realism after a certain level of increase". After completing the tracing, the beam tracing results of the OTIR prism in different states of the DMD can be obtained directly. (Figure 9).